

Effective photodarkening suppression in Yb-doped fiber lasers by visible light injection

Original

Effective photodarkening suppression in Yb-doped fiber lasers by visible light injection / Piccoli, R.; Robin, T.; Brand, T.; Klotzbach, U.; Taccheo, S.. - In: OPTICS EXPRESS. - ISSN 1094-4087. - ELETTRONICO. - 22:7(2014), pp. 7638-7643. [10.1364/OE.22.007638]

Availability:

This version is available at: 11583/2867150 since: 2021-01-25T22:44:19Z

Publisher:

Optical Society of America

Published

DOI:10.1364/OE.22.007638

Terms of use:

This article is made available under terms and conditions as specified in the corresponding bibliographic description in the repository

Publisher copyright

(Article begins on next page)

Effective photodarkening suppression in Yb-doped fiber lasers by visible light injection

Riccardo Piccoli,^{1,2} Thierry Robin³, Thomas Brand⁴, Udo Klotzbach,⁵ and Stefano Taccheo^{1,*}

¹College of Engineering, Swansea University, Singleton Park, Swansea SA2 8PP, UK

²On leave from: Facoltà di Ingegneria, Università degli Studi di Pavia, via Ferrata 3, Pavia 27100, Italy

³iX Fiber S.A.S., Rue Paul Sabatier, F-22300 Lannion, France

⁴DILAS, Galileo Galilei Straße 10, D-55129 Mainz, Germany

⁵Fraunhofer IWS, Winterbergstraße 28, D – 01277 Dresden, Germany

*s.taccheo@swansea.ac.uk

Abstract: Al-silicate fibers have excellent manufacturing quality. Unfortunately, high-Yb doping concentration may be limited by severe losses induced by photodarkening phenomenon. In this paper we demonstrate for the first time that Al-silicate Yb-doped fibers with high-inversion and doping concentration above 1 wt% can be successfully used by implementing a simple optical bleaching scheme. A co-injection into the active fiber of a few mW of light at around 550 nm wavelength successfully eliminates almost all photodarkening induced losses. We demonstrate operation at above 90% of the pristine output power level in several lasers with up to 30% Yb ions in the excited state. These results may allow to use Yb-doped Al-silicate fibers with doping level increased by one order of magnitude. Finally, we provide a comprehensive picture of main parameters affecting photobleaching performance and, to the best of our knowledge, we report the first quantitative measurement of the Ytterbium excited state absorption cross-section in the visible range.

©2014 Optical Society of America

OCIS codes: (140.3510) Lasers, fiber; (140.3615) Lasers, ytterbium; (160.5690) Rare-earth-doped materials.

References and links

1. D. J. Richardson, J. Nilsson, and W. A. Clarkson, "High power fiber lasers: current status and future perspective," *J. Opt. Soc. Am. B* **27**(11), B63 (2010).
2. J. Koponen, M. Söderlund, H. J. Hoffman, D. A. V. Kliner, J. P. Koplow, and M. Hotoleanu, "Photodarkening rate in Yb-doped silica fibers," *Appl. Opt.* **47**(9), 1247–1256 (2008).
3. R. Paschotta, J. Nilsson, P. R. Barber, J. E. Caplen, A. C. Tropper, and D. C. Hanna, "Lifetime quenching in Yb-doped fibers," *Opt. Commun.* **136**(5-6), 375–378 (1997).
4. S. Jetschke, U. Röpke, S. Unger, and J. Kirchhof, "Characterization of photodarkening processes in Yb doped fibers," *Proc. SPIE* **7195**, 71952B (2009).
5. S. Taccheo, H. Gebavi, A. Monteville, O. Le Goffic, D. Landais, D. Mechin, D. Tregoeat, B. Cadier, T. Robin, D. Milanese, and T. Durrant, "Concentration dependence and self-similarity of photodarkening losses induced in Yb-doped fibers by comparable excitation," *Opt. Express* **19**(20), 19340–19345 (2011).
6. S. Jetschke, S. Unger, U. Röpke, and J. Kirchhof, "Photodarkening in Yb doped fibers: experimental evidence of equilibrium states depending on the pump power," *Opt. Express* **15**(22), 14838–14843 (2007).
7. H. Gebavi, S. Taccheo, D. Milanese, A. Monteville, O. Le Goffic, D. Landais, D. Mechin, D. Tregoeat, B. Cadier, and T. Robin, "Temporal evolution and correlation between cooperative luminescence and photodarkening in ytterbium doped silica fibers," *Opt. Express* **19**(25), 25077–25083 (2011).
8. S. Jetschke and U. Röpke, "Power-law dependence of the photodarkening rate constant on the inversion in Yb doped fibers," *Opt. Lett.* **34**(1), 109–111 (2009).
9. P. Laperle, L. Desbiens, K. Le Foulgoc, M. Drolet, P. Deladurantaye, A. Proulx, and Y. Taillon, "Modeling the photodegradation of large mode area Yb-doped fiber power amplifiers," *Proc. SPIE* **7195**, 71952C (2009).
10. J. J. Koponen, M. J. Söderlund, H. J. Hoffman, and S. K. T. Tammela, "Measuring photodarkening from single-mode ytterbium doped silica fibers," *Opt. Express* **14**(24), 11539–11544 (2006).
11. M. N. Zervas, F. Ghiringhelli, M. K. Durkin, and I. Crowe, "Distribution of photodarkening-induced loss in Yb-doped fiber amplifiers," *Proc. SPIE* **7914**, 79140L (2011).

12. T. Eidam, C. Wirth, C. Jauregui, F. Stutzki, F. Jansen, H. J. Otto, O. Schmidt, T. Schreiber, J. Limpert, and A. Tünnemann, "Experimental observations of the threshold-like onset of mode instabilities in high power fiber amplifiers," *Opt. Express* **19**(14), 13218–13224 (2011).
13. S. Rydberg and M. Engholm, "Experimental evidence for the formation of divalent ytterbium in the photodarkening process of Yb-doped fiber lasers," *Opt. Express* **21**(6), 6681–6688 (2013).
14. J. Kirchhof, S. Unger, A. Schwuchow, S. Jetschke, V. Reichel, M. Leich, and A. Scheffel, "The influence of Yb²⁺ ions on optical properties and power stability of ytterbium doped laser fibers," *Proc. SPIE* **7598**, 75980B (2010).
15. K. E. Mattsson, "Photo darkening of rare earth doped silica," *Opt. Express* **19**(21), 19797–19812 (2011).
16. S. Yoo, C. Basu, A. J. Boyland, C. Sones, J. Nilsson, J. K. Sahu, and D. Payne, "Photodarkening in Yb-doped aluminosilicate fibers induced by 488 nm irradiation," *Opt. Lett.* **32**(12), 1626–1628 (2007).
17. P. Jelger, M. Engholm, L. Norin, and F. Laurell, "Degradation-resistant lasing at 980 nm in a Yb/Ce/Al-doped silica fiber," *J. Opt. Soc. Am. B* **27**(2), 338 (2010).
18. M. Engholm and L. Norin, "Preventing photodarkening in ytterbium-doped high power fiber lasers; correlation to the UV-transparency of the core glass," *Opt. Express* **16**(2), 1260–1268 (2008).
19. S. Jetschke, S. Unger, M. Leich, and J. Kirchhof, "Photodarkening kinetics as a function of Yb concentration and the role of Al codoping," *Appl. Opt.* **51**(32), 7758–7764 (2012).
20. J. Kirchhof, S. Unger, S. Jetschke, A. Schwuchow, M. Leich, and V. Reichel, "Yb doped silica based laser fibers: correlation of photodarkening kinetics and related optical properties with the glass composition," *Proc. SPIE* **7195**, 71950S (2009).
21. S. Jetschke, S. Unger, A. Schwuchow, M. Leich, and J. Kirchhof, "Efficient Yb laser fibers with low photodarkening by optimization of the core composition," *Opt. Express* **16**(20), 15540–15545 (2008).
22. A. Monteil, S. Chausseant, G. Alombert-Gogot, N. Gaumer, J. Obriot, S. J. L. Ribeiro, Y. Messaddeq, A. Chiasera, and M. Ferrari, "Clustering of rare earth in glasses, aluminum effect: experiments and modeling," *J. Non-Cryst. Solids* **348**, 44–50 (2004).
23. A. D. G. Chávez, A. V. Kir'yanov, Y. O. Barmenkov, and N. N. Il'ichev, "Reversible photo-darkening and resonant photobleaching of ytterbium-doped silica fiber at in-core 977-nm and 543-nm irradiation," *Laser Phys. Lett.* **4**(10), 734–739 (2007).
24. H. Gebavi, S. Taccheo, D. Tregoa, A. Monteville, and T. Robin, "Photobleaching of photodarkening in ytterbium doped aluminosilicate fibers with 633 nm irradiation," *Opt. Mater. Express* **2**(9), 1286 (2012).
25. I. Manek-Hönninger, J. Boulet, T. Cardinal, F. Guillen, S. Ermeneux, M. Podgorski, R. Bello Doua, and F. Salin, "Photodarkening and photobleaching of an ytterbium-doped silica double-clad LMA fiber," *Opt. Express* **15**(4), 1606–1611 (2007).
26. H. Gebavi, S. Taccheo, L. Lablonde, B. Cadier, T. Robin, D. Méchin, and D. Tregoa, "Mitigation of photodarkening phenomenon in fiber lasers by 633 nm light exposure," *Opt. Lett.* **38**(2), 196–198 (2013).
27. R. Piccoli, H. Gebavi, S. Taccheo, L. Lablonde, B. Cadier, T. Robin, A. Monteville, O. Le Goffic, D. Landais, D. Méchin, D. Milanese, T. Brand, "Photodarkening mitigation in Yb-doped fiber lasers by 405 nm irradiation," *Advanced Solid State Lasers (ASSL) AM2A.6* (2013).
28. M. Engholm, S. Rydberg, and K. Hammarling, "Strong excited state absorption (ESA) in Yb-doped lasers," *Proc. SPIE* **8601**, 86010P (2013).
29. R. Piccoli, D. Méchin, T. Robin, and S. Taccheo, "Lifetime reduction due to photodarkening phenomenon in ytterbium-doped fibers and rate equation term," *Opt. Lett.* **38**(21), 4370–4373 (2013).
30. S. Jetschke, A. Schwuchow, S. Unger, M. Leich, M. Jäger, and J. Kirchhof, "Deactivation of Yb³⁺ ions due to photodarkening," *Opt. Mater. Express* **3**(4), 452–458 (2013).
31. D. Faucher and R. Vallee, "Real-time photobleaching and stable operation at 204 mW of a Tm : ZBLAN blue fiber laser," *IEEE Photon. Technol. Lett.* **19**(2), 112–114 (2007).

1. Introduction

In recent years, Yb-doped Al-Silicate fiber lasers and amplifiers have been increasingly employed in many applications [1]. Unfortunately their efficiency may be compromised at high-doping level by photodarkening (PD) phenomenon which induces extra loss when Yb³⁺ ions are inverted [2–9]. The PD induced extra loss is distributed over a broad absorption band from ultra-violet to IR region [10,11] affecting operation of 1 μm fiber laser and amplifier. In addition, this phenomenon involves not only power degradation over time but it may also affect beam quality via mode instability threshold degradation [12]. This effect is not completely clear yet and different theories have been proposed in order to understand the underlying microscopic process: the formation of divalent ytterbium [13,14]; "1^{1/2}" bond color center (CC) [15] or related to ODC (Oxygen Deficiency Center) defects in aluminosilicate fibers where Oxygen bonds are modified [16]. For these reasons, in the recent years several groups made a huge effort in order to investigate, model and mitigate this phenomenon. Suppression or mitigation of PD in silica fibers has been achieved by co-doping the active fiber with cerium [17] or phosphorus [18] and in general by controlling the glass core composition [19–22]. However, changes in chemical composition could lead to changes

in the manufacturing process and on refractive index, impacting on guiding properties, as well as on the shape of absorption spectrum. Therefore, efforts were devoted to investigate removal of PD losses in aluminosilicate fibers. Experiments using UV-VIS light were able to successfully remove a significant percentage of PD induced loss with partial [23,24] or complete [25] bleaching of a doped fiber.

In past works we decided to investigate photobleaching (PB) of laser devices by simultaneous injection of a bleaching radiation into the active fiber during laser operation [26,27]. We found 633 nm radiation [26] cannot provide effective bleaching. This may be due to a set of high energy defects needing higher energy photons to be bleached [24]. Further, we noticed that blue light at 405 nm while can bleach higher energy PD defects it cannot effectively penetrate a laser cavity longer than few millimeters due to very high excited state absorption (ESA) [27]. This is also confirmed by a previous spectroscopy investigation where ESA in the UV interval was reported [28]. In addition we measured a detrimental PD induced by ground-state-absorption (GSA) of 405-nm radiation [27]. We also found, for our set of fibers, that PD does not significantly affect Yb lifetime value [29], despite in a previous case degradation was reported [30]. We were therefore convinced a laser can operate at the almost pristine level once PD loss are eliminated by an optimized bleaching wavelength, as previously achieved in Tm-doped ZBLAN fiber lasers [31]. This technique requires a simple injection scheme similar to the one used to inject the visible pointing beam light in commercial lasers. In this work, we do not enter into the debate of the PD mechanism but we present a first proposal to effectively remove PD loss in Yb-doped Al-silicate fiber laser. The proposed set-up and the optimization of the bleaching wavelength is based on an experimental investigation of factors involved in the process and in particular on the first, to the best of our knowledge, quantitative measurement of the ESA cross-section.

2. Experimental

Figure 1(a) shows the set-up used to measure the Yb ESA cross-section.

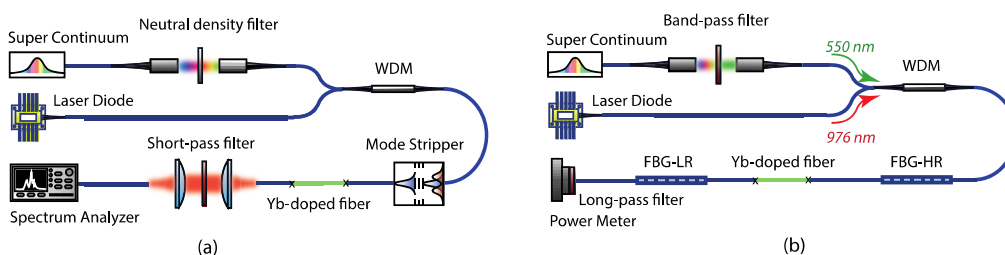


Fig. 1. (a) Set-up used to measure ESA cross-section. (b) Set-up used to test bleaching of an operating laser.

To measure the visible ESA spectrum we used a 30-MHz repetition-rate picosecond continuum source with white spectrum from 480 nm wavelength to over 1 micron. The white laser source was free-space attenuated by using a neutral-density filter to reduce the power at the μW level for the spectroscopic measurement and then filtered (short-pass filter with cut-off wavelength of 800 nm). The continuum spectrum and the 976 nm pump were coupled into the active fiber under test using a custom wavelength division multiplexer (WDM, visible/976 nm). Since WDM output fiber (HI1060) was not single-mode (SM) at visible wavelengths, we introduced a mode-stripper stage in order to remove the light propagating in the cladding. As test fiber we used a single-mode fiber with 1.35 wt% ($1.12 \cdot 10^{26}$ ions/ m^3) Yb-doping concentration and 3.2 wt% Al^{3+} content. The fiber had a 6.6 μm core diameter and was spliced to the mode-stripper. We measured the visible transmitted light by collimating and filtering (short-pass) the active fiber output in order to remove the pump radiation before refocusing it into the optical spectrum analyzer (OSA) input fiber as shown in Fig. 1(a). This set-up allowed us to measure the transmitted spectrum in the 480 nm - 750 nm wavelength interval

in two different conditions: with the pump radiation on or off. The injected pump power of 240 mW was able to ensure constant saturated inversion all along the fiber under test [5]. The corresponding ESA cross-section was calculated, assuming a constant inversion all along the fiber, by using the following formula:

$$\sigma_{ESA}(\lambda) = \frac{-\ln \left[\frac{P_{w,p}(\lambda) - P_p(\lambda)}{P_w(\lambda)} \right]}{L_{Yb} \cdot N_{tot} \cdot N_2} \quad (1)$$

where: L_{Yb} was the length of the active fiber equal to 4.6 cm; N_{tot} the doping concentration equal to $1.12 \cdot 10^{26}$ ions/m³; N_2 the percentage of ions in the excited state, equal to 46% ($N_2 = 0.46$) in the case of saturated inversion; $P_{w,p}(\lambda)$ the power transmitted when the fiber was pumped and $P_w(\lambda)$ the power transmitted with un-pumped fiber. The term $P_p(\lambda)$ takes into account the visible luminescence emitted from excited Yb ions due to the pumping process [7]. This luminescence is added to the transmitted spectrum and therefore has to be subtracted to avoid ESA cross section underestimation. This latter term was evaluated measuring the emitted spectrum with only pump on (no white light injected) and the same saturated inversion level. This method allows to normalized the result by the fiber length since we operated at constant saturated inversion all along the fiber. Finally, time measurement and white-probe power were sufficiently short (few seconds) and low not to affect the ESA cross-section measurement by PD and PB phenomena respectively [5].

Figure 2(a) shows the calculated ESA cross-section from 480 nm, the lower limit of the white source spectrum, to 750 nm. Considering the uncertainty on the uniform saturated inversion, the stability of coupling condition and the OSA noise level, the cross section value is estimated to be within -5% to $+10\%$ of the reported data. The larger underestimation is due to our assumption of constant saturated inversion. From Fig. 2(a) we can expect by linear extrapolation an absorption of about 86% at 405 nm over 1 cm of our fiber which confirms the results observed in our previous work [27]. The extrapolated value is in good agreement with [28]. The set of data suggests the optimum PB wavelength should maximize the interplay of three effects: 1) photons with enough energy to erase even the highest energy PD defects (likely with wavelength below 600 nm); 2) avoid PD generation via GSA; 3) minimize ESA to effectively compensate PD all along the active fiber (likely use of photons with 500 nm).

To investigate optimum PB condition we investigated the effect of varying the PB wavelength in the 510 nm–570 nm interval and the active fiber length. Figure 1(b) shows the used set-up. The white spectrum was free-space filtered with a band-pass filter (40 nm at Full-width half-maximum) centered at different peak wavelength. Two customized FBGs, centered at 1070 nm with reflectivity peaks of 99% (High-Reflectivity, HR) and 41% (Low-Reflectivity, LR), were spliced at both ends of the active fiber. The 1070 nm lasing wavelength was chosen due to its negligible absorption cross-section which leads to gain and amount of PD loss to depend only on the number of inverted Yb³⁺ ions for easier comparison of different configuration [5]. The laser output power temporal evolution was monitored and a long-pass filter was used in front of the power meter to remove both the residual pump power and PB light.

First, we tested different fiber lasers injecting bleaching radiation at different wavelengths but using a similar active fiber length of about 4.5 cm. To quantify bleaching effectiveness we observed the power drop due to PD when the bleaching radiation was injected during laser operation. We recorded the initial and final level when an equilibrium state, due to dynamic interplay of PD and PB, was reached. For a comparable bleaching power of 4 mW we found a maximum difference of final value of less than 10% for bleaching wavelength in the 510 nm–570 nm interval, the best result being obtained at around 550 nm. The comparable power drop can be explained by similar penetration depth (similar ESA cross section values) and similar phonon energy. In term of absolute power drop we found a maximum decrease of 20% with

respect to the initial pristine laser power level. A significantly better result compared with the ones previously obtained using either 405 nm or 633 nm radiation [26,27].

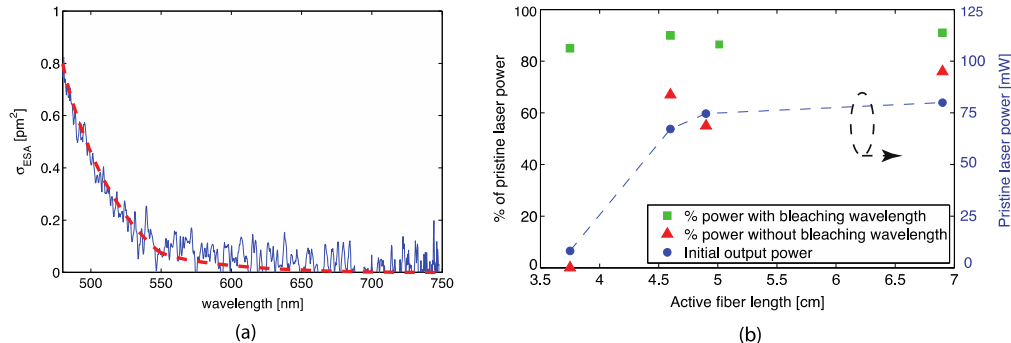


Fig. 2. (a) Measured excited state absorption (ESA) cross-section. A strong absorption from excited state starts for wavelength shorter than 550 nm. (b) Percentage of 1070-nm laser power drop versus active fiber length. Squares and triangles shows percentage of power degradation with and without bleaching radiation injected, respectively.

To better quantify the effectiveness of PB we performed a second set of experiments using 550-nm as PB wavelength and varying the active fiber length from about 4.5 cm to 7 cm. Since the output coupling is constant the variation of fiber length affects the inversion level and therefore the amount of induced PD loss [2,3] and the impact of ESA. In all tests the injected power level of 550-nm radiation was in the range of 6 mW to 8 mW. Figure 2(b) shows the percentage of laser power drop at 1070 nm for different active fiber length. We first measured the laser output power at 1070 nm in pristine condition (time zero, circles in Fig. 2(b)) and then we let the laser power evolve with pump power on and the bleaching radiation coupled. When the equilibrium was reached, we measured again the power level (squares in Fig. 2(b)). After, we switched off the bleaching radiation and we let the power evolve until a final equilibrium stage is reached (triangles). Figure 2(b) shows that in all cases with inversion close or less than 30% we were able to operate the laser at 90% or above of the initial power level. If we now compare these results with the ones previously achieved for laser operating in similar condition we record a power drop less than 10% using 550 nm bleaching radiation instead of over 45% using either 405 nm [27] or 630 nm [26] radiation.

The experiment with the 3.75 cm long fiber was performed to test a worst case scenario. We induced an extra loss with an intentionally bad splicing between the active fiber and the output coupler. This ensured to work with more than 40% of inverted ions, very close to the maximum allowed inversion. Without PB radiation the laser was unable to compensate the extra loss induced by PD and went below threshold stopping to operate. Yet, we were able to keep the laser running at 85% of its initial power level with about 8 mW of injected bleaching power. This worst case confirms the possibility to remove a significant percentage of the PD induced loss even when the laser is operating at very high inversion.

To provide more insight on the benefit of PB we performed a set of experiment using a 4.9 cm-long active fiber as gain medium. Figure 3(a) shows the laser characteristic in the three different situations as in Fig. 2(b). As expected, by using about 8 mW of light at 550 nm, we were able to keep the laser slope efficiency and threshold at almost their pristine values with a power level drop of only 5%. When we switched off the 550-nm bleaching radiation the laser power dropped down until reaching a new equilibrium level with a threshold increased from ~21 mW to ~31 mW and a power drop of about 45%. This indicates power drop is mostly due to slope efficiency decrease than laser threshold increase. We also observed the possibility to recover the laser at almost the same equilibrium level by switching on again the bleaching radiation, similarly as done in [27]. To further appreciate the effectiveness of PB, Fig. 3(b) shows the laser output power temporal evolution with and without PB. In this case we made two equal cavities and we compared the power evolution starting in both cases from a pristine

situation. Note the two initial pristine power levels were about 2 mW different and were scaled to the same level for sake of clarity. It is worth to note in case of PB most of power drop occurs in the first 20 minutes, suggesting possible factory pre-burning.

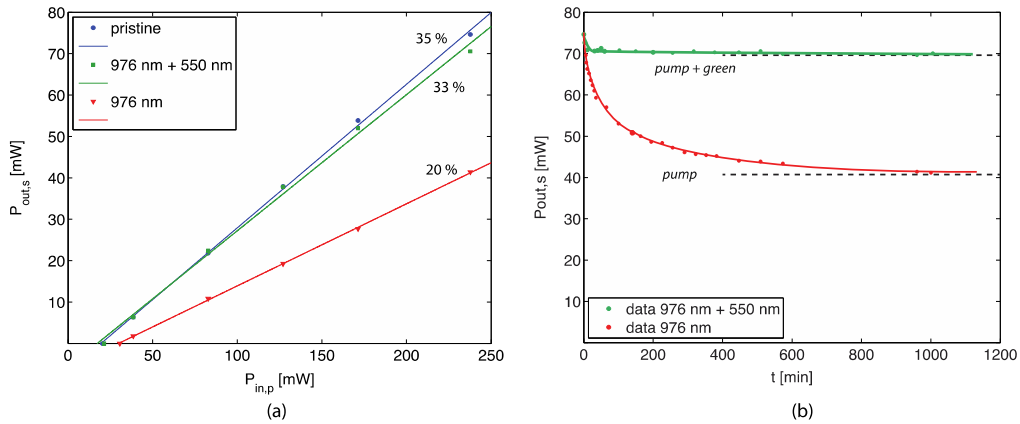


Fig. 3. (a) Output laser power $P_{out,s}$ versus input pump power $P_{in,p}$ in each equilibrium level: (blue) initial status, (green) 976 nm and 550 nm together, (red) only 976 nm. (b) Laser output power temporal evolution with (green line) and without (red line) bleaching radiation at 550 nm. In all experiments we used a 4.9 cm long active fiber.

Optimum PB wavelength depends on many laser parameters, including fiber length, inversion, doping level. A detailed investigation is needed case by case and is out of the aim of this paper, aimed to provide general guidelines. Pumping scheme has also an impact. Photobleaching power scales with the core area for injection into the core and with the cladding area injection into cladding using double-cladding (DC) fibers. However DC scheme will allow shorter PB wavelengths since the lower absorption per unit of length.

3. Conclusion

In conclusion, we present an effective yet simple way to operate a laser using standard Al-silicate fibers with high doping level over 10^{26} ions/m³ and high population inversion of 30% and above. This technique requires a simple injection scheme similar to the one used to inject the pointing beam red light in commercial lasers and could be a practical solution to successfully mitigate PD in highly-doped fiber lasers and amplifiers. In order to shed more light on the bleaching phenomenon, we measured, for the first time to the best of our knowledge, the excite-state absorption cross-section in the visible wavelength interval and we optimized the PB wavelength playing with the three main parameters: photon energy, ground-state and excites-state absorption: optimum bleaching wavelength would range from 510 nm for short cavity laser (few centimeters/a few tens of centimeters) to 560 nm/570 nm for meter long lasers. A set of experiment were performed by injecting 550-nm radiation in different fiber lasers and we were able to keep the output power level within 90% of its initial value.

Acknowledgment

This project was funded by the FP7 LIFT (Leadership in Fiber Technology) Project (Grant #228587).